Acta Neurochirurgica (2019) 161:2513–2519
https://doi.org/10.1007/s00701-019-04097-8

ORIGINAL ARTICLE - NEUROSURGICAL ANATOMY

Quantitative measurement of the surgical freedom for anterior communicating artery complex—a comparative study between the frontotemporal pterional and supraorbital craniotomy; a laboratory study

Cheng-Mao Cheng [1,2] · Aclan Dogan [3]

Received: 19 July 2019 / Accepted: 7 October 2019 / Published online: 24 October 2019

Abstract

Objective To quantitatively measure surgical degree of freedom (SDF) to the anterior communicating artery (AComA) complex via removal of the orbital rim. Comparisons of SDF quadrants were made between a supraorbital and standard frontotemporal pterional craniotomy according to the surgeons' geometric microscope compass-based views.

Methods Eleven latex-injected formalin-fixed cadaveric heads; 14 sides (eight unilateral and three bilateral) were dissected. Standard frontotemporal pterional and subsequent supraorbital craniotomy approaches were conducted in each specimen. Point "0" was allocated as a point 1 cm distal to the ipsilateral A1 and A2 junction of AComA. The tip of a 10-cm long pointer was used to locate point 0. The base of the pointer stick was maneuvered outside the craniotomy in eight compass directions, with the most peripheral points expressed as target points 1–8. The center of this octagon was attributed point C. A pyramid was established by connecting the points 0, C, and 2 neighboring target points. A frameless stereotaxic instrument was used as a three-dimensional digitizer to measure pyramid volume. Each neighboring two pyramids form a hexagonal cone and was expressed as a surgical freedom quadrant (cm^3). The quadrants are depicted counterclockwise (surgeons view) as orbital-nasal, vertex-nasal, vertex-temporal, and orbital-temporal.

Results Total SDF obtained via supraorbital and pterional approaches were 122.8 ± 109.66 and 159.94 ± 93.65, respectively (mean ± SD cm^3; supraorbital < pterional by 30.2%). Supraorbital to pterional, in the orbital-nasal quadrant was 21.9 ± 35.5 and 13.04 ± 8.7, vertex-nasal 31.3 ± 28.5 and 16.7 ± 13.7, vertex-temporal 39.5 ± 42.14 and 60.4 ± 4.7, and orbital-temporal 30.14 ± 42.14 and 70.01 ± 42.14, respectively (mean ± SD cm^3). In the vertex-nasal quadrant, the supraorbital approach provides a 47.3% increase in SDF compared to the standard frontotemporal pterional craniotomy approach.

Conclusion Given that the AComA complex is located more nasally and the surgeon's view is more vertex, we propose that a supraorbital craniotomy allows a more contralateral portion of the AComA complex to be visualized during dissection.

Keywords Frontotemporal pterional · Anterior communicating artery · Supraorbital · Cadaver

This article is part of the Topical Collection on *Neurosurgical Anatomy*

✉ Aclan Dogan
dogana@ohsu.edu

[1] Department of Neurosurgery, Neurological Institute, Taichung Veterans General Hospital, Taichung, Taiwan

[2] Department of Neurological Surgery, Tri-Service General Hospital, National Defense Medical Center, Taipei Taiwan

[3] Department of Neurological Surgery, Oregon Health & Science University, CH8N, 3303 SW Bond Avenue, Portland, OR 97239, USA

Abbreviations

AComA	Anterior communicating artery
SD	Standard deviation
PTE	Standard frontotemporal pterional
SDF	Surgical degree of freedom
SUP	Supraorbital

Introduction

Standard frontotemporal pterional (PTE) craniotomy is a mainstay surgical approach for a broad pathologic spectrum

in the vicinity of the cavernous sinus, sella, parasellar, and subfrontal regions[18]. Anterior communicating artery (AComA) aneurysms are the most common type of cerebral aneurysms: 30–37% of all intracranial aneurysms [14] and are successfully treated via a PTE craniotomy [8, 15].

However, due to anterolateral corridor access to the AComA complex, PTE craniotomy can obscure both the contralateral A1 and the recurrent artery of Heubner, and thus, additional gyrus rectus resection can be necessary to clearly visualize the aneurysm neck. This raises concerns of eliciting new neuropsychological changes [2]. Anterior skull base approaches with an orbital rim osteotomy have previously reported satisfactory clinical outcomes [1, 2, 7, 13]. Anatomically, the AComA complex sits cranially and medially to the skull opening when the head is secured in usual fashion. Surgical degree of freedom (SDF) is one of the major end points of skull base exposure and represents the total degree of maneuverability attained by the surgeon within an entire surgical area; certain areas may be more or less accessible, and consequently, beneficial gains in SDF can be neutralized by other SDF, and vice versa.

Surgical degree of freedom can be categorized as two measurements: (1) an axial or vertical angle expressed as angular degree units and (2) summation of triangles above the skull base expressed as geometric area. These SDF measurements allow surgeons to conceptualize dissections in a given direction. However, when placing a clip for AcomA aneurysm while the surgical microscope is fixed, one needs to estimate medial or caudal space in an attempt to spare small branches surrounding the AComA complex. There is paucity of information available related to skull base SDF expressed as geometric areas.

Therefore, the goal of this anatomical cadaveric study was to determinate whether SDF can be expressed as a unit of volume and divided into quadrants. A quantitative comparison of the spatial exposure of surgical degree of freedom via supraorbital (SUP) and PTE craniotomy was undertaken based on geometric microscope compass-based views.

Methods

Dissections

Fourteen cadaveric head sides were dissected (unilateral in eight and bilateral in three) in a skull base laboratory. Specimens were perfused and fixed with phenol and 5% formalin solution. The main arteries and veins of specimens were injected with red and blue latex dye, respectively.

The cadaveric heads were secured in a head holder and were dissected with the aid of regular and microsurgical instruments under the supplement of a surgical microscope (Zeiss OPMI, Carl Zeiss Surgical, Inc.) and a high-speed drill system (Micromax, Anspach Companies, Inc.).

The cadaveric heads were fixed on a head frame and turned to the contralateral side by 45° with the malar eminence in the uppermost position. A bicoronal incision was made beginning less than 1 cm anterior to the tragus on the level of zygomatic arch and carried superiorly above the superior temporal line at the level of coronal suture and across the midline by 4–5 cm to the intersection with contralateral middle pupillary line. To minimize brain texture between specimens, we conducted two sequential approaches on the same side of a specimen: (1) PTE and after data acquisition, the skull was reconstructed for (2) SUP. A 1-cm-width brain spatula was placed in the same area of subfrontal gyrus during each sequential dissection to minimize intragroup bias. The SUP and PTE approaches (Fig. 1) were as previously described [4].

Frontotemporal pterional approach

A bur hole was made 1 cm above the zygomatic root, and the bone cut was directed superiorly to the intersection of the superior temporal line and the coronal suture line and was turned medially to join the medial margin of keyhole bone cut, and the frontotemporal bone flap was disarticulated [4].

Supraorbital approach

The pterional flap was reconstructed with steel wires. A new bone cut was started from the anatomical keyhole to the intersection of superior temporal line and coronal suture line and extended medially to join the bone cut made in the pterional bone cut. With an additional orbital osteotomy, the supraorbital bone flap was completed [4].

Data analysis

A system of frameless stereotaxy (StealthStation, Medtronic Sofamor Danek, Memphis, TN) was used to determine three dimensional Cartesian coordinates (x, y, and z). A reference arm was secured to a bench table, and specimens were fixed in a head holder. Throughout measurement course, the relationship between the reference arm, specimen, and brain spatula remained constant. The tip of navigation bar functioned as digital localizer that transmitted the x, y, and z coordinates to the navigation system's central processor. A 10-cm-length straight dissector was used as a reference bar with a dimple on the basal end. During the measurement, the tip of the reference bar was pointed to the point zero (point 0), which is defined as a point 1 cm distal to the A1–A2 junction on the A2 segment (Fig. 2), and the base of pointer dissector move toward eight directions (north, northeast, east, southeast, south, southwest, west, and northwest). In each direction, the target point was defined as the most peripheral point in a given

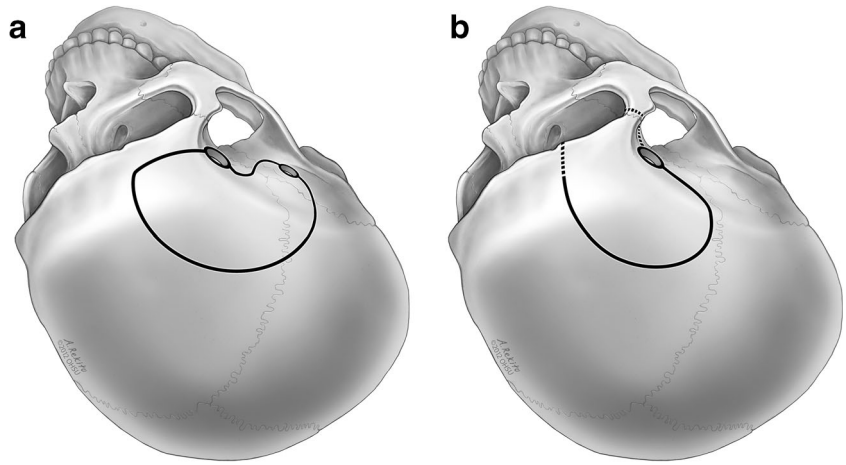

Fig. 1 Illustration of the surgical views of frontotemporal pterional craniotomy (**a**) and supraorbital craniotomy (**b**), with permission from OHSU

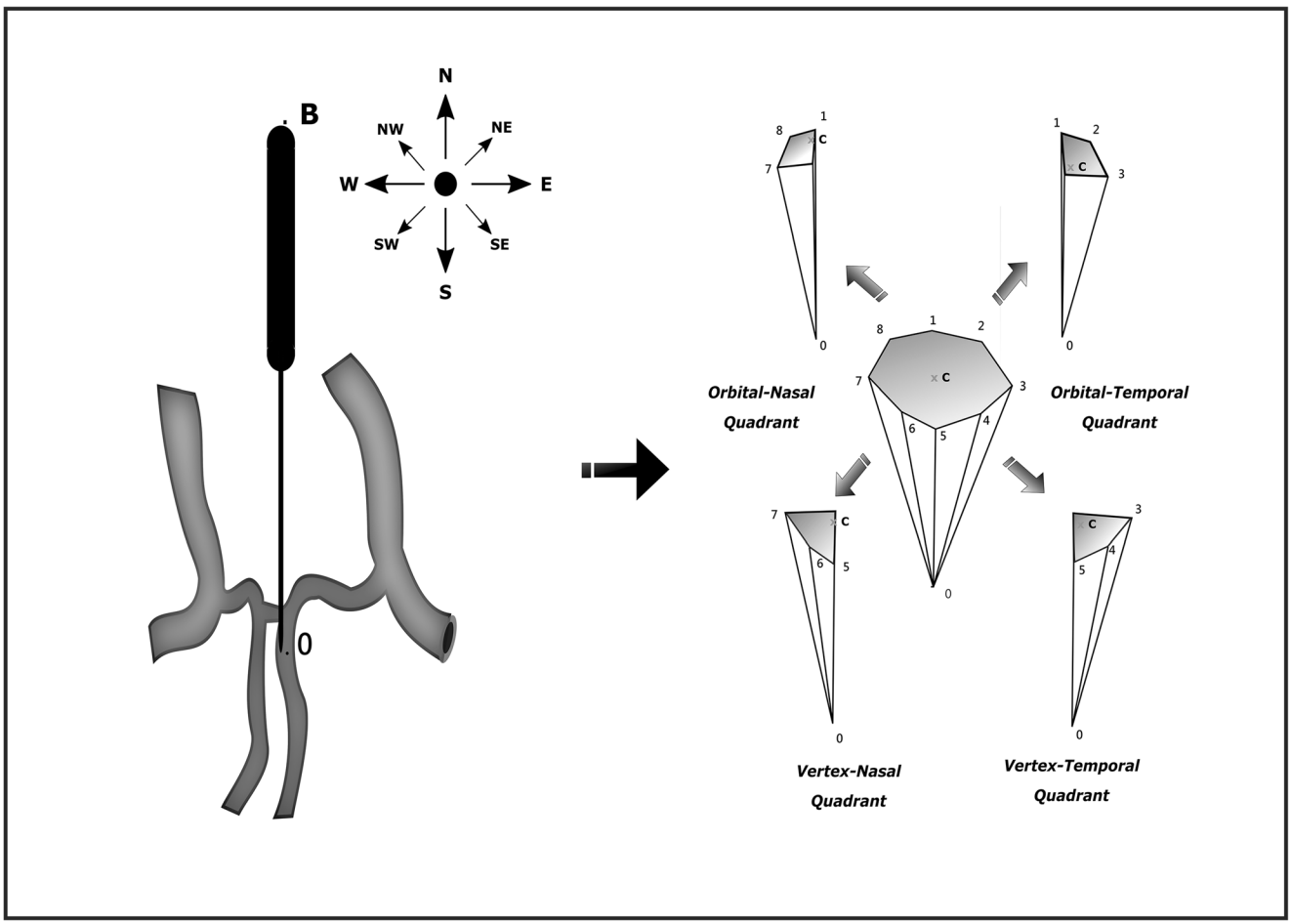

Fig. 2 Illustration showing the three-dimensional data acquisition. The tip of a 10-cm-length straight dissector is directed on the point 0, which is the point 1 cm distal to the junction of ipsilateral A1A2 junction of anterior communicating artery complex. Point B is the base of this dissector and moved as most eccentrically as it goes within the craniotomy in eight cardinal and intercardinal directions (north, northeast, east, southeast, south, southwest, west, and northwest). Each peripheral most point was annotated as target points 1–8, whereas the center of these eight target points was depicted as point C. By joining point 0, point C, and two neighboring target points, we will have a triangular pyramid. For instance, pyramid 0-C-1-2 and pyramid 0-C2-3 represent the tetrahedron pyramid respectively in the northeast direction, and these two triangular pyramids are merged as a hexagonal pyramid. For better view of surgeons' perception during dissection, these hexagonal pyramids are depicted as surgical freedom quadrants in the orbital-temporal, vertex-temporal, vertex-nasal, and orbital-nasal quadrants

direction. The target point was defined as points 1 to 8 in sequence and recorded with digitalizing the dimple of the basal end of the reference bar. An octagon can be drawn by connecting these eight target points, with an orthocenter defined as "point C". Eight pyramids were generated by connecting point 0, point C, and two neighboring two target points. All datasets were recorded in a spreadsheet (Microsoft Excel; Microsoft Corp., Redmond, WA) pyramid vertices, point 1 = (x1, y1, z1), point 2 = (x2, y2, z2), point C = (x3, y3, z3), and point 0 = (x4, y4, z4). To highlight the comparisons, surgical freedom quadrant was defined as the hexagonal cone by way of joining two pyramids in their quadrant of compass orientation: orbital-nasal, vertex-nasal, vertex-temporal, and orbital-temporal (Fig. 3; Table 1).

Results

Surgical degree of freedom

The total SDF offered by via SUP and PTE craniotomy for the AComA complex was 122.8 ± 109.66 versus 159.94 ± 93.65 cm^3 respectively. SUP surgical freedom was < PTE by 30.2%.

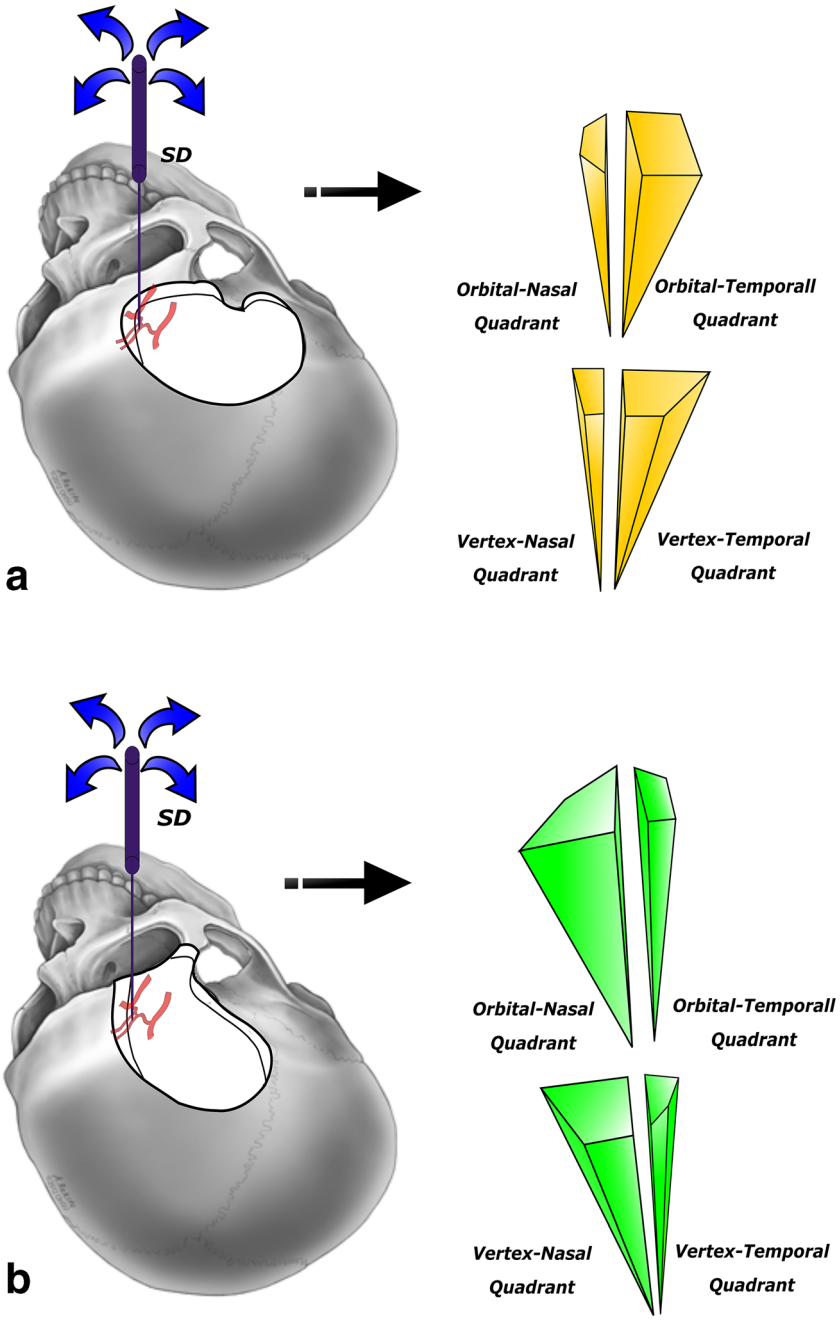

Fig. 3 **a** Illustration depicting the surgical freedom quadrants for the PTE craniotomy. The straight dissector was presented as SD, with its tip positioned in point 0 and its base, point B, (see Fig. 2) move peripherally toward the compass direction. Four surgical freedom quadrants, orbital-nasal, vertex-nasal, vertex-temporal, and orbital-temporal (see also in Fig. 2), were constructed as hexagonal pyramids and expressed in yellow color. **b** Illustration depicting the surgical freedom quadrants for the SUP craniotomy. The four surgical freedom quadrants, orbital-nasal, vertex-nasal, vertex-temporal, and orbital-temporal, were expressed in green color for comparison with those for PTE craniotomy

Table 1 Comparison of surgical freedom quadrants of anterior communicating artery complex via the PTE and SUP craniotomy

Volume calculation $\frac{1}{6}\begin{bmatrix} x1 & y1 & z1 & 1 \\ x2 & y2 & z2 & 1 \\ x3 & y3 & z3 & 1 \\ x4 & y4 & z4 & 1 \end{bmatrix}$

Surgical freedom quadrants (cm^3)

	PTE	SUP	(S/P)Δ%
Orbital-nasal	13.04 ± 8.7	21.9 ± 35.5	40.3
Vertex-nasal	16.7 ± 13.7	31.3 ± 28.5	47.3
Vertex-temporal	60.4 ± 4.7	39.5 ± 42.14	− 53.0
Orbital-temporal	70.01 ± 42.14	30.14 ± 42.14	− 132.2
Total	159.94 ± 93.65	122.8 ± 109.66	− 30.2

Values represent the mean ± SD

SUP supraorbital craniotomy; *PTE* pterional approach, *(S/P)Δ%* percentage gain in surgical freedom quadrant with SUP craniotomy comparing that with PTE craniotomy

In the orbital-nasal quadrant, SUP versus PTE for the AComA complex was 21.9 ± 35.5 versus 13.04 ± 8.7 cm^3; vertex-nasal, 31.3 ± 28.5 versus 16.7 ± 13.7cm^3; vertex-temporal, 39.5 ± 42.14 versus 60.4 ± 4.7 cm^3; orbital-temporal, 30.14 ± 42.14 versus 70.01 ± 42.14 cm^3.

In the vertex-nasal quadrant, SUP provides 47.3% increase in surgical freedom compared to that of PTE (Table 1).

Discussion

Surgical degree of freedom is one of the major end point results in many comparative quantitative studies for a variety of different neurosurgical approaches. Figueiredo et al. and Andaluz et al. used the vertical and axial angle to express the SDF obtained in the orbitopterional, orbitozygomatic, and mini-supraorbital approaches [2, 5, 6]. Spektor et al., Horgan et al., and Hsu et al., used perimeter and horizontal plane to represent SDF in mm^2 units [9, 10, 16]. Baretta et al. advocated a novel working area (mm^2 units), by summation of six triangles above the sellar and perisellar regions to express surgical freedom via supraorbital and transorbital mini craniotomies [3]. These methods comprehensively convey the notion of surgeon directed surgical instrument movement within the boundary of cranial openings. However, the measurements are indirect, and it is difficult to conceptualize space and volume.

In this cadaveric laboratory study, we utilized geometric pyramid volumes to represent SDF in cm^3 (Table 1). This allows surgeons to conceptualize direct spatial volume in which a surgical instrument can be moved within a surgical space. We also present SDF as surgical freedom quadrants (compass-based), to represent estimates of SDF obtained in different microscopic views.

We quantitatively analyzed the geometric relationship between the surgical region of interest, the AComA complex, and cranial openings. We measured SDF volumetrically as cm^3 as opposed to horizontally or vertically as an angle of attack [2, 6]. Surgical freedom was divided in four quadrants mimicking the microscope light: orbital-nasal, vertex-nasal, vertex-temporal, and orbital-temporal. Overall, total SDF with SUP was less than PTE (by − 30.2%); however, vertex-nasal quadrant SDF was greater in SUP than in PTE (by 47.3%) (Table 1). Anatomically, the AComA complex resides on more nasal and vertex portion in relation to the center of the surgical field in skull base. With more SDF in the vertex-nasal quadrant, the SUP craniotomy has the clinical implication of allowing more contralateral A1 and A2 arteries and its branches to be visualized, which is advantageous in planning aneurysm clipping. The percentage of surgical freedom for various quadrants from SUP to PTE craniotomy is depicted in Fig. 4. The change of quadrant SDF is + 40.3% in orbital-nasal and + 47.3% in vertex-nasal quadrant, while the change of quadrant SDF is negative: − 132.2% in orbital-temporal and − 53.0% in vertex-temporal quadrant (Fig. 5). These data demonstrate that the quadrant of SDF relates to the orientation of skull flap. Although the bone flap size of SUP craniotomy is indeed smaller, due to a more medial and orbital location, it

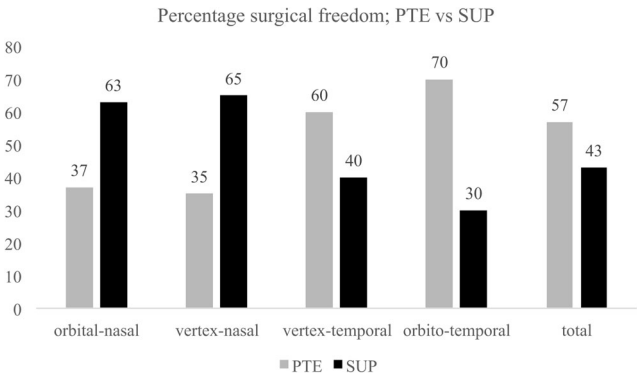

Fig. 4 Percentage of surgical freedom for various quadrants; frontotemporal pterional craniotomy vs. supraorbital craniotomy

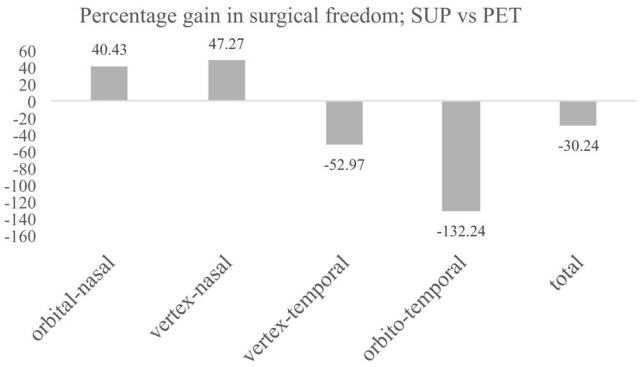

Fig. 5 Percentage gain in surgical freedom for various quadrants; supraorbital craniotomy vs. frontotemporal pterional craniotomy

allows surgeons to visualize a more medial and more orbital cranial portion of the AComA. Therefore, the contralateral branches of A1 and A2 arteries can be more reliably observed with less brain retraction, and the rectal gyrus better preserved. Andaluz et al. reported a series of 40 patients who underwent AComA aneurysmal clipping surgery via the orbitopterional craniotomy [2], which included orbital rim removal. Their results showed that three (7.5%) patients had rectal gyrus resection, with no incidences of frontobasal hypodensities on postoperative computed tomographic scans, and no sylvian fissure dissection was required [2]. Petraglia et al. described a similar unilateral subfrontal approach in 28 patients with anterior communicating artery aneurysms, whereby the orbital rim was preserved. Contrary to the Andaluz study, the rectal gyrus was resected in 57% of cases [12].

The AComA complex sites centrally in the interhemispheric fissure. Suzuki et al. described a bifrontal interhemispheric approach to better observe AcomA complex [17]. However, this approach is technically demanding when the aneurysmal dome is superior and when preservation of olfactory function is attempted during subfrontal dissection. Jane et al. described a supraorbital approach to treat AComA aneurysms [11]. Riina et al. described an orbitozygomatic approach for large or giant AComA aneurysms and a modified orbitozygomatic approach for smaller aneurysms [13]. Andaluz et al. described an orbitopterional approach and Petraglia et al. a unilateral subfrontal approach. Collectively, for these approaches, the craniotomy in comparison to the standard pterional craniotomy is more nasal in orientation [2, 12]. Thus, it is logical to expect a more direct frontal view of the AComA aneurysm by selecting a lower and more medial craniotomy.

Here, we used a supraorbital craniotomy with orbital rim osteotomy as a laboratory-based model. This bone flap ensures the most caudal extension to the periorbita tissue, and nasal protraction medially to the supraorbital foramen/or notch by 0.5 cm, which often blocks access to the frontal sinus. We present a novel spatial expression of SDF in cm^3 with division into four surgical freedom quadrants. Clinically, if the pathology of the area of interest is more nasal and orbital, it is reasonable to expect more surgical freedom quadrants when the corresponding skull base parts are resected. For example, an orbital rim resection to remove more nasal and orbital of skull base parts. The vertex-temporal and orbital-temporal surgical freedom was noticeably smaller for the SUP approach than the PTE approach. This could be because the SUP skull flap is medial to the frontal process of the zygomatic bone and includes no temporal bone elements. Since the AComA complex is located nasally in the cistern of lamina terminalis, the SUP craniotomy allows for a more direct corridor to the complex, while the microscopic light beam is in position during clipping, and also provides a substantial volume of surgical freedom in the nasal part of the complex.

This simulated laboratory-based study has several limitations. First, the consistency of the formalin-fixed and latex-injected brains varies among specimens. To minimize the intragroup bias, we performed two craniotomies in each specimen while a brain spatula was used to hold up the frontal basal lobe in the same location during the dissections. Second, the contents in the cistern of lamina terminalis also differ; some are filled with melt fluid while others are tangled with leaked latex dye. Both will nevertheless affect intergroup data regularity. Third, the allocation of the tip (point 0; Fig. 2) of the 10-cm straight dissector was selected as a point 1 cm distal to the ipsilateral A1–A2 junction to simulate the distal control of A2. The base (point B; Fig. 2) of the dissector moves in a compass sequence. The AComA complex is small compared to the skull flap opening, and only one allocation of point 0 is required for each measurement. The calculated surgical freedom quadrant is a conceptually reverse pyramid volume. The clinical implication is that one can visualize corner space while clipping in a fixed microscopic view. Our data did not support surgical freedom in the dissection planes above the skull base where the microscope light beam is constantly changing. Andaluz et al. and Beretta et al. use a summation of triangles model in the dissection planes to calculate working area as a tool of surgical freedom [2, 3].

A thorough understanding of AComA complex pathology and sound surgical experience are important aspects of safe outcomes and patient satisfaction. The SUP craniotomy is an option in the surgeon's armamentarium if surgical freedom is a goal in clipping the AComA complex.

Conclusions

In this study, we present SDF as four surgical freedom quadrants according to the surgeons' view under light microscopy. With resection of the orbital rim and compared to the PTE approach, the SUP approach allows surgeons to visualize more medial part of AComA complex.

Acknowledgments The authors thank Drs. Akio Noguchi, Gregory J. Anderson, Frank H. Hsu, Sean O. McMenomey, and Johnny B. Delashaw for their contributions in the cadaver laboratory, and Shirley McCartney, Ph.D., for her editorial assistance.

Compliance with ethical standards

Conflict of interest The authors declare that they have no conflict of interest.

Ethical approval Cadaveric heads were provided by OHSU's Body Donation Program with an Enrolment Form for Individual Donating to OHSU's Whole Body Donation Program in place.

References

1. Ammirati M, Spallone A, Ma J, Cheatham M, Becker D (1993) An anatomicosurgical study of the temporal branch of the facial nerve. Neurosurgery 33:1038–1044. https://doi.org/10.1227/00006123-199312000-00012
2. Andaluz N, van Loveren HR, Keller JT, Zuccarello M (2003) Anatomic and clinical study of the orbitopterional approach to anterior communicating artery aneurysms. Neurosurgery 52:1140–1149. https://doi.org/10.1227/01.neu.0000057834.83222.9f
3. Beretta F, Andaluz N, Chalaala C, Bernucci C, Salud L, Zuccarello M (2010) Image-guided anatomical and morphometric study of supraorbital and transorbital minicraniotomies to the sellar and perisellar regions: comparison with standard techniques. J Neurosurg 113:975–981. https://doi.org/10.3171/2009.10.Jns09435
4. Cheng CM, Noguchi A, Dogan A, Anderson GJ, Hsu FP, McMenomey SO, Delashaw JB Jr (2013) Quantitative verification of the keyhole concept: a comparison of area of exposure in the parasellar region via supraorbital keyhole, frontotemporal pterional, and supraorbital approaches. J Neurosurg 118:264–269. https://doi.org/10.3171/2012.9.Jns09186
5. Figueiredo EG, Deshmukh P, Zabramski JM, Preul MC, Crawford NR, Siwanuwatn R, Spetzler RF (2005) Quantitative anatomic study of three surgical approaches to the anterior communicating artery complex. Oper Neurosurg 56:397–405. https://doi.org/10.1227/01.neu.0000156549.96185.6d
6. Figueiredo EG, Deshmukh V, Nakaji P, Deshmukh P, Crusius MU, Crawford N, Spetzler RF, Preul MC (2006) An Anatomical evaluation of the mini-supraorbital approach and comparison with standard craniotomies. Oper Neurosurg 59:ONS-212-ONS-220. https://doi.org/10.1227/01.neu.0000223365.55701.f2
7. Fujitsu K, Kuwabara T (1986) Orbitocraniobasal approach for anterior communicating artery aneurysms. Neurosurgery 18:367–369. https://doi.org/10.1227/00006123-198603000-00023
8. Hernesniemi J, Dashti R, Lehecka M, Niemelä M, Rinne J, Lehto H, Ronkainen A, Koivisto T, Jääskeläinen JE (2008) Microneurosurgical management of anterior communicating artery aneurysms. Surg Neurol 70:8–28. https://doi.org/10.1016/j.surneu.2008.01.056
9. Horgan MA, Anderson GJ, Kellogg JX, Schwartz MS, Spektor S, McMenomey SO, Delashaw JB (2000) Classification and quantification of the petrosal approach to the petroclival region. J Neurosurg:108–112. https://doi.org/10.3171/jns.2000.93.1.0108
10. Hsu FPK, Anderson GJ, Dogan A, Finizio J, Noguchi A, Liu KC, McMenomey SO, Delashaw JB (2004) Extended middle fossa approach: quantitative analysis of petroclival exposure and surgical freedom as a function of successive temporal bone removal by using frameless stereotaxy. J Neurosurg:695–699. https://doi.org/10.3171/jns.2004.100.4.0695
11. Jane JA, Park TS, Pobereskin LH, Winn RH, Butler AB (1982) The supraorbital approach: technical note. Neurosurgery 11:537–542. https://doi.org/10.1227/00006123-198210000-00016
12. Petraglia A, Moravan M, Jahromi B, Maurer P, Srinivasan V, Coriddi M, Vates G (2011) Unilateral subfrontal approach to anterior communicating artery aneurysms: a review of 28 patients. Surg Neurol Int 2:124. https://doi.org/10.4103/2152-7806.85056
13. Riina HA, Lemole GM, Spetzler RF (2002) Anterior communicating artery aneurysms. Neurosurgery 51:993–996. https://doi.org/10.1227/00006123-200210000-00026
14. Sekhar LN, Natarajan SK, Britz GW, Ghodke B (2007) Microsurgical management of anterior communicating artery aneurysms. Oper Neurosurg 61:ONS273–ONS292. https://doi.org/10.1227/01.neu.0000303980.96504.d9
15. Solomon RA (2001) Anterior communicating artery aneurysms. Neurosurgery 48:119–123. https://doi.org/10.1227/00006123-200101000-00021
16. Spektor S, Anderson GJ, McMenomey SO, Horgan MA, Kellogg JX, Delashaw JB (2000) Quantitative description of the far-lateral transcondylar transtubercular approach to the foramen magnum and clivus. J Neurosurg:824–831. https://doi.org/10.3171/jns.2000.92.5.0824
17. Suzuki J, Mizoi K, Yoshimoto T (1986) Bifrontal interhemispheric approach to aneurysms of the anterior communicating artery. J Neurosurg:183–190. https://doi.org/10.3171/jns.1986.64.2.0183
18. Vishteh AG, Marciano FF, David CA, Baskin JJ, Spetzler RF (1998) The pterional approach. Oper Tech Neurosurg 1:39–49. https://doi.org/10.1016/s1092-440x(98)80007-8